Top quark pair production and decay at a polarized photon collider

A. Brandenburg [a,*]**, Z. G. Si** [b,†]

[a]DESY-Theorie, 22603 Hamburg, Germany
[b]Department of Physics, Shandong University, Jinan, Shandong 250100, China

Abstract:

Top quark pair production by (polarized) $\gamma\gamma$ collisions offers an interesting testing ground of the Standard Model and its extensions. In this Letter we present results for differential cross sections of top quark pair production and decay including QCD radiative corrections. We take into account the full dependence on the top quark spins. We give analytic and numerical results for single and double differential angular distributions of $t\bar{t}$ decay products which are due to top quark polarizations and spin correlations in the intermediate state.

Keywords: photon collider, top quarks, QCD corrections, polarization, spin correlations

arXiv:hep-ph/0503153v3 2 Apr 2005

I. Introduction

At a future linear lepton collider, backscattered laser light may provide very high-energy photons [1], which would allow for a very interesting physics program [2, 3]. In particular, top quark pair production is possible with large rates in (un)polarized photon photon fusion. The measurement of the process $\gamma\gamma \to t\bar{t}X$ is an important test of the Standard Model (SM). The first order QCD corrections to this process have already been calculated and found to be large [4–7]. The electroweak virtual plus soft-photonic $O(\alpha)$ corrections are also known [8]. This process will also provide information on possible anomalous $\gamma t\bar{t}$ couplings [9, 10] without contributions from $Zt\bar{t}$ couplings present in e^+e^- collisions.

Once the Higgs boson is discovered, it will be of primary importance to determine whether its properties are as predicted within the SM. In this respect, the process $\gamma\gamma \to t\bar{t}X$ may play an important role. For example, heavy quark production in polarized $\gamma\gamma$ collisions will help to determine the parity of the Higgs boson produced as a resonance and decaying into top quark pairs [6, 7]. In particular, if a Higgs boson is no CP eigenstate, spin correlations of the top quark pairs will help to probe the scalar and pseudoscalar couplings of the Higgs boson to the top quark [11, 12].

For this kind of studies, predictions for top quark pair production and decay at a photon collider must be as precise as possible within the SM. In particular, the spin state of the intermediate $t\bar{t}$ pair must be taken into account. (The role of the top quark polarization in probing the $t\bar{t}$ threshold dynamics in $\gamma\gamma$ collisions was discussed in [13]).

The purpose of this paper is therefore to study the processes

$$\gamma\gamma \to t\bar{t}X \to \ell + \ell' + X, \quad \ell + \text{ jets} + X, \quad \text{all jets}, \tag{I.1}$$

where ℓ stands for a charged lepton, with polarized photons from backscattered laser beams. We include QCD radiative corrections and take into account polarization and spin correlation effects of the intermediate $t\bar{t}$ pairs.

Leading order results and QCD corrections for the cross section and for top quark spin observables in the process $\gamma\gamma \to t\bar{t}X$ are summarized in sections II and III. Numerical results to order $\alpha^2\alpha_s$ for the effective lepton collider cross section and for several decay distributions are given in section IV.

II. Kinematics and leading order results

The production of top quark pairs by photon scattering at leading order $\alpha^2\alpha_s^0$ is described by the reaction

$$\gamma(p_1, \lambda_1) + \gamma(p_2, \lambda_2) \to t(k_1, s_t) + \bar{t}(k_2, s_{\bar{t}}). \tag{II.1}$$

Here, p_1, p_2, k_1 and k_2 denote the momenta of the particles, λ_1 and λ_2 are the helicities of the photons, and the vectors s_t and $s_{\bar{t}}$ describe the spins of top quark and antiquark. These fulfil the relations

$$s_t^2 = s_{\bar{t}}^2 = -1 \quad \text{and} \quad k_1 \cdot s_t = k_{\bar{t}} \cdot s_{\bar{t}} = 0. \tag{II.2}$$

In the (anti)top rest frame the spin of the (anti)top is described by a unit vector $\hat{s}_t$ ($\hat{s}_{\bar{t}}$). We choose the specific rest frames that are obtained by a rotation-free Lorentz boost from the zero momentum frame of the $t\bar{t}$ quarks ($t\bar{t}$-ZMF). Both the $t\bar{t}$-ZMF and the t and $\bar{t}$ rest frames will be used to construct spin

observables from the final state momenta of the $t\bar{t}$ decay products. We use the $t\bar{t}$-ZMF rather than the c.m. frame of the colliding high-energy photons, since the latter system is probably more difficult to reconstruct experimentally. For the $2 \rightarrow 2$ process of Eq. (II.1), the two frames coincide.

The differential cross section for the process of Eq. (II.1) can be written as follows:

$$d\sigma(\lambda_1, \lambda_2, s_t, s_{\bar{t}}) = \frac{N}{2s_{\gamma\gamma}}|M_0|^2 d\Gamma_2, \tag{II.3}$$

where the two-particle phase space measure is denoted by $d\Gamma_2$, $s_{\gamma\gamma} = (p_1 + p_2)^2$ and $N = 3$ is the number of colours. A simple calculation gives:

$$
\begin{aligned}
|M_0|^2 &= \frac{16\alpha^2 Q_t^4 \pi^2}{(1 - \beta^2 z^2)^2} \Big\{ A_0 + B_0\left[p_1 \cdot (s_t + s_{\bar{t}})\right] + B_0|_{\lambda_1 \leftrightarrow \lambda_2}\left[p_2 \cdot (s_t + s_{\bar{t}})\right] \\
&+ C_0(s_t \cdot s_{\bar{t}}) + D_0(p_1 \cdot s_t)(p_2 \cdot s_{\bar{t}}) + D_0|_{z \rightarrow -z}(p_2 \cdot s_t)(p_1 \cdot s_{\bar{t}}) \Big\}
\end{aligned}
\tag{II.4}
$$

with

$$A_0 = 1 + 2\beta^2(1 - z^2) - \beta^4\left[1 + (1 - z^2)^2\right] + \lambda_1\lambda_2\left[1 - 2\beta^2(1 - z^2) - \beta^4 z^2(2 - z^2)\right], \tag{II.5}$$

$$B_0 = \frac{4m}{s_{\gamma\gamma}}\left[\lambda_1(1 - 2\beta^2 + \beta^2 z^2) + \lambda_2(1 - \beta^2 z^2)\right], \tag{II.6}$$

$$C_0 = 1 - 2\beta^2 + \beta^4\left[1 + (1 - z^2)^2\right] + \lambda_1\lambda_2\left[1 - 2\beta^2 + \beta^4 z^2(2 - z^2)\right], \tag{II.7}$$

$$D_0 = -\frac{4(1 + \beta z)(1 - z^2)(1 - \lambda_1\lambda_2)\beta^2}{s_{\gamma\gamma}}. \tag{II.8}$$

Here, $Q_t = 2/3$, m is the top quark mass,

$$\beta = \sqrt{1 - \frac{4m^2}{s}}, \tag{II.9}$$

and z is the cosine of the scattering angle in the $t\bar{t}$-ZMF, i.e. $z = \hat{\mathbf{p}}_\gamma \cdot \hat{\mathbf{k}}$, where $\hat{\mathbf{p}}_\gamma$ ($\hat{\mathbf{k}}$) is the direction of one of the photons (of the top quark) in that frame.

III. NLO results for $\gamma\gamma \rightarrow t\bar{t}X$

In this section we present results for the inclusive reaction

$$\gamma\gamma \rightarrow t\bar{t}X \tag{III.1}$$

to order $\alpha^2\alpha_s$. Apart from the cross section we study observables that depend on the spins of the top quark and antiquark. For polarized photons, observables of the form

$$O^s = 2\mathbf{S}_t \cdot \hat{\mathbf{a}} \tag{III.2}$$

2

can have non-zero expectation values. Here, $\hat{\mathbf{a}}$ is an arbitrary reference direction and $\mathbf{S}_t$ is the top quark spin operator. The expectation value of O^s is related to a single spin asymmetry:

$$\langle O^s \rangle = \frac{\sigma(\uparrow) - \sigma(\downarrow)}{\sigma(\uparrow) + \sigma(\downarrow)}, \tag{III.3}$$

where the arrows on the right-hand side refer to the spin state of the top quark with respect to the quantization axis $\hat{\mathbf{a}}$. We will consider here two choices for $\hat{\mathbf{a}}$,

$$
\begin{aligned}
\hat{\mathbf{a}} &= \hat{\mathbf{k}} &&\text{(helicity basis)}, \\
\hat{\mathbf{a}} &= \hat{\mathbf{p}} &&\text{(beam basis)},
\end{aligned}
\tag{III.4}
$$

where $\hat{\mathbf{k}}$ denotes the direction of the top quark in the $t\bar{t}$-ZMF and $\hat{\mathbf{p}}$ is the direction of the lepton beam coming from the left in that frame, which coincides to good approximation with the direction of one of the high-energy photons. Top quark polarization perpendicular to the plane spanned by $\hat{\mathbf{p}}$ and $\hat{\mathbf{k}}$ is induced by absorptive parts in the one-loop amplitude. This effect is, however, quite small ($\sim$ a few percent) [14].

Analogous observables may of course be defined for the top antiquark.

Apart from the above single spin observables, we also consider observables of the form

$$O^d = 4(\mathbf{S}_t \cdot \hat{\mathbf{a}})(\mathbf{S}_{\bar{t}} \cdot \hat{\mathbf{b}}). \tag{III.5}$$

Here, $\hat{\mathbf{a}}$ and $\hat{\mathbf{b}}$ are arbitrary reference directions and $\mathbf{S}_{\bar{t}}$ is the top antiquark spin operator. The expectation value of O^d is related to a double spin asymmetry:

$$\langle O^d \rangle = \frac{\sigma(\uparrow\uparrow) + \sigma(\downarrow\downarrow) - \sigma(\uparrow\downarrow) - \sigma(\downarrow\uparrow)}{\sigma(\uparrow\uparrow) + \sigma(\downarrow\downarrow) + \sigma(\uparrow\downarrow) + \sigma(\downarrow\uparrow)}. \tag{III.6}$$

For the reference directions we will consider here

$$
\begin{aligned}
\hat{\mathbf{a}} &= -\hat{\mathbf{b}} = \hat{\mathbf{k}}, \\
\hat{\mathbf{a}} &= \hat{\mathbf{b}} = \hat{\mathbf{p}}.
\end{aligned}
\tag{III.7}
$$

Finally, we also present results for the observable

$$\tilde{O}^d = \frac{4}{3}\mathbf{S}_t \cdot \mathbf{S}_{\bar{t}}. \tag{III.8}$$

The above double spin asymmetries $\langle O^d \rangle$ and $\langle \tilde{O}^d \rangle$ have also proved useful for an analysis of spin correlations of top quark pairs in hadronic collisions [15].

The NLO cross section for the reaction $\gamma\gamma \to t\bar{t}X$ may be written in terms of two scaling functions:

$$\sigma(\hat{s}, m, \lambda_1, \lambda_2) = \frac{\alpha^2 Q_t^4}{m^2} \left[c^{(0)}(\rho, \lambda_1, \lambda_2) + 4\pi\alpha_s c^{(1)}(\rho, \lambda_1, \lambda_2) \right]. \tag{III.9}$$

Likewise, the unnormalized expectation values of the above spin observables are of the form

$$\sigma\langle O_a \rangle = \frac{\alpha^2 Q_t^4}{m^2} \left[d_a^{(0)}(\rho, \lambda_1, \lambda_2) + 4\pi\alpha_s d_a^{(1)}(\rho, \lambda_1, \lambda_2) \right], \tag{III.10}$$

3

where $a = 1$ corresponds to the observable $\tilde{O}^d$ defined in Eq. (III.8), $a = 2(3)$ to the observable O^d defined in Eq. (III.5) in the helicity (beam) basis, and $a = 4(5)$ corresponds to the single spin observable O^s defined in Eq. (III.2) in the helicity (beam) basis. The variable ρ is defined as

$$\rho = \frac{4m^2}{s_{\gamma\gamma}}. \tag{III.11}$$

The lowest order scaling functions $c^{(0)}$ and $d_a^{(0)}$ can be computed analytically. We use the following auxiliary functions, which vanish in the limit $\beta = \sqrt{1-\rho} \to 0$:

$$
\begin{aligned}
\ell_1 &= \frac{1}{\beta}\left[\ln(x) + 2\beta\right], \\
\ell_2 &= \frac{1}{\beta^3}\left[\ln(x) + 2\beta + \frac{2}{3}\beta^3\right], \\
\ell_3 &= \frac{1}{\beta^5}\left[\ln(x) + 2\beta + \frac{2}{3}\beta^3 + \frac{2}{5}\beta^5\right],
\end{aligned} \tag{III.12}
$$

where $x = (1-\beta)/(1+\beta)$. We then obtain:

$$
\begin{aligned}
c^{(0)}(\rho,\lambda_1,\lambda_2) &= N\pi\beta\rho\left\{1 + \rho - \rho^2 + \lambda_1\lambda_2 - \left[1 + \rho - \frac{\rho^2}{2} - \lambda_1\lambda_2\right]\ell_1\right\}, \\
d_1^{(0)}(\rho,\lambda_1,\lambda_2) &= -\frac{N\pi\beta\rho}{3}\left\{1 + \rho + \rho^2 + (1+2\rho)\lambda_1\lambda_2 + \left[1 - \frac{\rho^2}{2} - (1+\rho)\lambda_1\lambda_2\right]\ell_1\right\}, \\
d_2^{(0)}(\rho,\lambda_1,\lambda_2) &= N\pi\beta\rho\left\{\frac{1 + 8\rho - 7\rho^2 + \rho^3 + (5 - 3\rho + \rho^2)\lambda_1\lambda_2}{3}\right. \\
&\quad \left. - \left[-1 + \rho - 2\rho^2 + \frac{\rho^3}{2} + \left(1 + \frac{\rho^2}{2}\right)\lambda_1\lambda_2\right]\ell_2\right\}, \\
d_3^{(0)}(\rho,\lambda_1,\lambda_2) &= N\pi\beta\rho\left\{-\frac{9 - 20\sqrt{\rho} - 6\rho + 14\rho^{3/2} + 29\rho^2 + 6\rho^{5/2} - 20\rho^3 + 3\rho^4}{15}\right. \\
&\quad + \frac{-21 - 20\sqrt{\rho} + 25\rho + 14\rho^{3/2} - 16\rho^2 + 6\rho^{5/2} - 3\rho^3}{15}\lambda_1\lambda_2 \\
&\quad + \left[-1 - 4\rho - \rho^2 - 2\sqrt{\rho} + \frac{\rho^3}{2} - 2\rho^{3/2} + \rho^{5/2}\right. \\
&\quad \left.\left. + \left(1 + 2\sqrt{\rho} + 3\rho + \frac{\rho^2}{2}\right)\lambda_1\lambda_2\right](1 - \sqrt{\rho})^2\ell_3\right\}, \\
d_4^{(0)}(\rho,\lambda_1,\lambda_2) &= N\pi\beta\rho\left\{\sqrt{1-\rho} - \frac{\rho}{2}\ln(x)\right\}(\lambda_1 + \lambda_2), \\
d_5^{(0)}(\rho,\lambda_1,\lambda_2) &= -N\pi\beta\rho\left\{\frac{1-\rho}{3}\left(1 - 6\sqrt{\rho} + \rho^{3/2}\right)\right. \\
&\quad \left. + \frac{1-\sqrt{\rho}}{2}\left(2 + 2\sqrt{\rho} + 3\rho - \rho^{3/2} - \rho^2\right)\ell_2\right\}(\lambda_1 - \lambda_2). \tag{III.13}
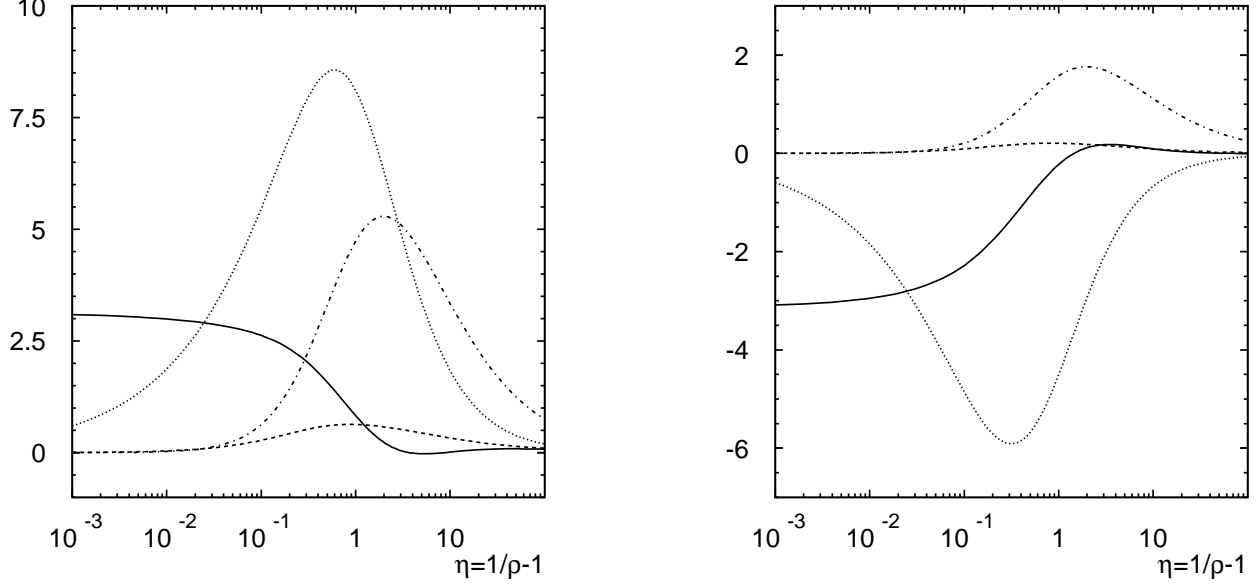\end{aligned}
$$

4

Figure 1: *Left: Scaling functions $c^{(0)}(\rho,1,1)$ (dotted), $c^{(0)}(\rho,1,-1)$ (dash-dotted), $c^{(1)}(\rho,1,1)$ (full), and $c^{(1)}(\rho,1,-1)$ (dashed). Right: Scaling functions $d_1^{(0)}(\rho,1,1)$ (dotted), $d_1^{(0)}(\rho,1,-1)$ (dash-dotted), $d_1^{(1)}(\rho,1,1)$ (full), and $d_1^{(1)}(\rho,1,-1)$ (dashed).*

The functions $c^{(1)}$ and $d_a^{(1)}$ are obtained by a numerical integration. The scaling functions for the spin-averaged cross section and all spin observables are plotted in Figs. 1-3 for different choices of the photon helicities as a function of

$$\eta = \frac{1}{\rho} - 1. \qquad (\text{III}.14)$$

The result for unpolarized photons can be inferred from

$$c^{(0),(1)}(\rho,0,0) = \frac{1}{2}\left[c^{(0),(1)}(\rho,1,1) + c^{(0),(1)}(\rho,1,-1)\right], \qquad (\text{III}.15)$$

$$d_{1,2,3}^{(0),(1)}(\rho,0,0) = \frac{1}{2}\left[d_{1,2,3}^{(0),(1)}(\rho,1,1) + d_{1,2,3}^{(0),(1)}(\rho,1,-1)\right], \qquad (\text{III}.16)$$

$$d_{4,5}^{(0),(1)}(\rho,0,0) = 0. \qquad (\text{III}.17)$$

As a check we compared our result for the functions $c^{(0),(1)}(\rho,0,0)$ with the results given in Fig. 2 of Ref. [4] and found perfect agreement. We further compared the functions $c^{(0),(1)}(\rho,1,\pm1)$ to the results given in Table 1 of Ref. [6]. After a trivial rescaling to account for the different conventions used in the definition of the scaling functions, we also found agreement.
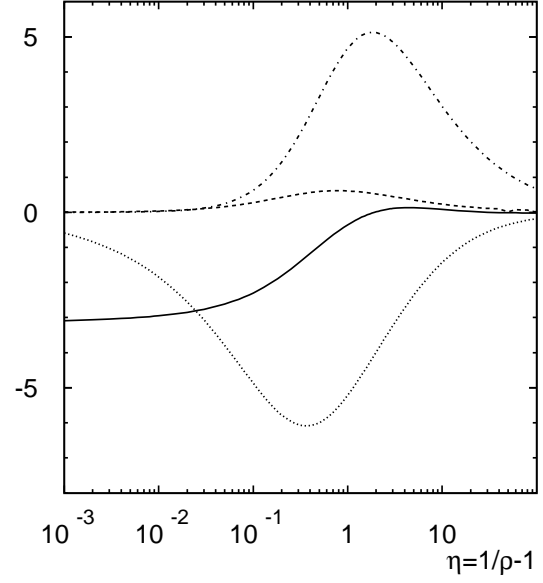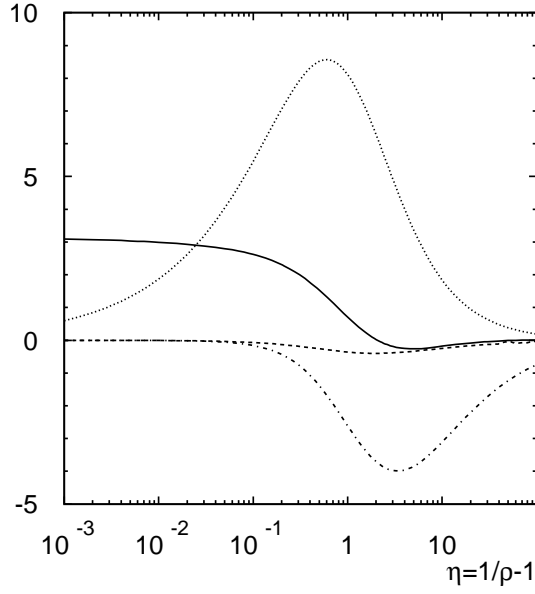
Figure 2: *Left: Scaling functions $d_2^{(0)}(\rho,1,1)$ (dotted), $d_2^{(0)}(\rho,1,-1)$ (dash-dotted), $d_2^{(1)}(\rho,1,1)$ (full), and $d_2^{(1)}(\rho,1,-1)$ (dashed). Right: Scaling functions $d_3^{(0)}(\rho,1,1)$ (dotted), $d_3^{(0)}(\rho,1,-1)$ (dash-dotted), $d_3^{(1)}(\rho,1,1)$ (full), and $d_3^{(1)}(\rho,1,-1)$ (dashed).*
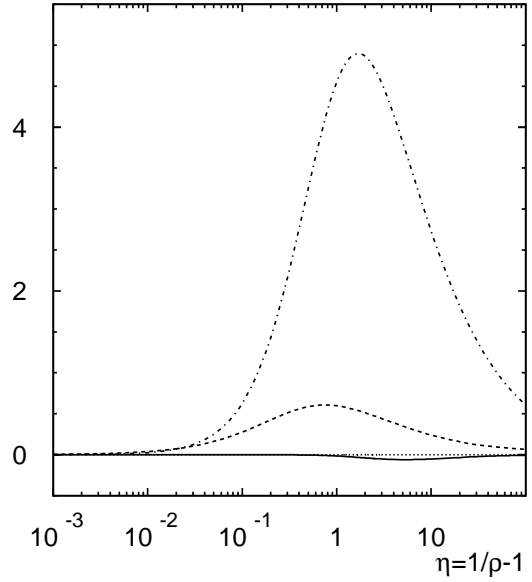

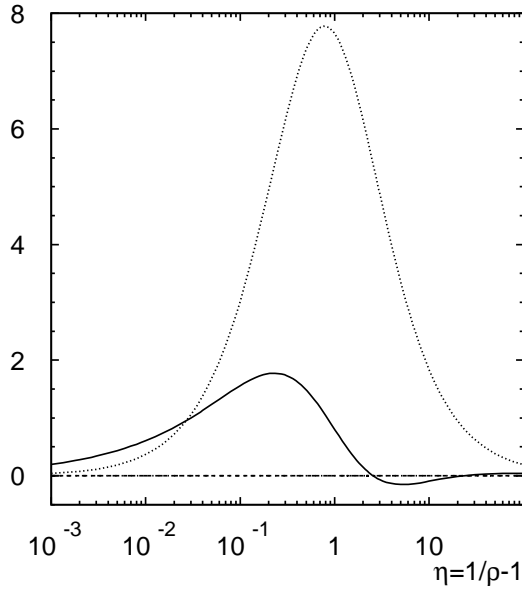Figure 3: *Left: Scaling functions $d_4^{(0)}(\rho,1,1)$ (dotted), $d_4^{(0)}(\rho,1,-1)$ (dash-dotted), $d_4^{(1)}(\rho,1,1)$ (full), and $d_4^{(1)}(\rho,1,-1)$ (dashed). Right: Scaling functions $d_5^{(0)}(\rho,1,1)$ (dotted), $d_5^{(0)}(\rho,1,-1)$ (dash-dotted), $d_5^{(1)}(\rho,1,1)$ (full), and $d_5^{(1)}(\rho,1,-1)$ (dashed).*

6

IV. Effective cross sections and spin observables

IV.1. The effective cross section for $\gamma\gamma \to t\bar{t}X$

The total $t\bar{t}$ cross section at a photon collider may be written at NLO QCD as (cf., e.g., [5])

$$\sigma_{t\bar{t}} = \frac{\alpha^2 Q_t^4}{m^2} \int_0^{y_{\max}} dy_1 \int_0^{y_{\max}} dy_2 f_\gamma^e(y_1, P_e, P_L) f_\gamma^e(y_2, P_e, P_L) \left\{ c^{(0)} + 4\pi\alpha_s c^{(1)} \right\}. \tag{IV.1}$$

The function $f_\gamma^e(y_1, P_e, P_L)$ is the normalized energy spectrum of the photons resulting from Compton backscattering of laser light off the high energy electron beam. It is explicitly given by:

$$f_\gamma^e(y, P_e, P_L) = \mathcal{N}^{-1} \left[\frac{1}{1-y} - y + (2r-1)^2 - P_e P_L xr(2r-1)(2-y) \right]. \tag{IV.2}$$

Here, $P_e(P_L)$ is the polarization of the electron (laser) beam, and y is the fraction of the electron energy in the c.m. frame transferred to the photon. It takes values in the range

$$0 \le y \le \frac{x}{x+1} \equiv y_{\max}, \tag{IV.3}$$

with

$$x = \frac{4E_L E_e}{m_e^2}, \tag{IV.4}$$

where $E_L(E_e)$ is the energy of the laser (electron) beam and m_e is the electron mass. In order to avoid the creation of an $e^+ e^-$ pair from the backscattered laser beam and the low energy laser beam, the maximal value for x is

$$x_{\max} = 2(1 + \sqrt{2}). \tag{IV.5}$$

For a beam energy $E_e = 250$ GeV, this leads to an optimal laser energy

$$E_L \approx 1.26 \text{ eV}, \tag{IV.6}$$

which will be used in the following numerical results. Finally,

$$r = \frac{y}{x(1-y)}. \tag{IV.7}$$

The normalization factor $\mathcal{N}$ in Eq. (IV.2) is determined by

$$\int_0^{y_{\max}} f_\gamma^e(y, P_e, P_L) dy = 1. \tag{IV.8}$$

The scaling functions $c^{(0),(1)}$ have to be evaluated at $\rho = 4m^2/(y_1 y_2 s_{ee})$ and for polarizations

$$\lambda_i = P_\gamma(y_i, P_e^{(i)}, P_L^{(i)}), \qquad i = 1, 2. \tag{IV.9}$$

Table 1: *Results for the effective cross section at $\sqrt{s_{ee}} = 500$ GeV.*

$(P_{e1}, P_{e2}; P_{L1}, P_{L2})$	$\sigma_{t\bar{t}}^{\mathrm{LO}}$ [fb]	$\sigma_{t\bar{t}}^{\mathrm{NLO}}$ [fb]	$K = \sigma_{t\bar{t}}^{\mathrm{NLO}}/\sigma_{t\bar{t}}^{\mathrm{LO}}$
$(0,0;0,0)$	49.81	76.44	1.53
$(0.85, 0.85; -1, -1)$	175.86	260.77	1.48
$(0.85, 0.85; +1, +1)$	15.96	26.89	1.68
$(0.85, -0.85; -1, +1)$	48.99	71.93	1.47

The function $P_\gamma(y, P_e, P_L)$ describes the degree of polarization of photons scattered with energy fraction y, which is given by

$$P_\gamma(y, P_e, P_L) = \frac{1}{\mathcal{N} f_\gamma^e(y, P_e, P_L)} \left\{ xrP_e \left[1 + (1-y)(2r-1)^2 \right] - (2r-1)P_L \left[\frac{1}{1-y} + 1 - y \right] \right\}. \quad \text{(IV.10)}$$

Numerical results for $\sigma_{t\bar{t}}$ are given in Table 1 for $\sqrt{s_{ee}} = 500$ GeV and different polarizations of the laser and electron beam. We use the values $m_t = 178$ GeV, $\alpha = 1/128$ and $\alpha_s(\mu = m_t) = 0.1$. The QCD corrections to $\sigma_{t\bar{t}}$ are quite large. This is because for $\sqrt{s_{ee}} = 500$ GeV most of the top quark pairs are produced close to threshold where the Coulombic β^{-1} singularity from soft gluons is important.

IV.2. Spin observables

The spin observables for $\gamma\gamma \to t\bar{t}X$ discussed in section III translate into observables built from the momenta of the $t\bar{t}$ decay products.

The single spin asymmetries (III.2) cause a nontrivial one-particle inclusive decay distribution of the form

$$\frac{1}{\sigma} \frac{d\sigma(\gamma\gamma \to a_1 + X)}{d\cos\theta_1} = \frac{1}{2}(1 + B_i \cos\theta_1). \quad \text{(IV.11)}$$

Here, θ_1 is the angle between the direction of a top quark decay product a_1 measured in the top quark rest frame and one of the reference directions $\hat{\mathbf{a}}$ defined in Eq. (III.4). The coefficient B_i, with $i = $ heli, beam for the helicity and beam bases, is determined by the top quark spin asymmetry (III.2) and by the so-called spin analysing power of the decay product a_1, which will be discussed below.

The double spin asymmetries (III.5) lead to a two-particle inclusive decay distribution of the following form:

$$\frac{1}{\sigma} \frac{d\sigma(\gamma\gamma \to a_1 a_2 + X)}{d\cos\theta_1 d\cos\theta_2} = \frac{1}{4}(1 + B_i \cos\theta_1 + \bar{B}_i \cos\theta_2 - C_i \cos\theta_1 \cos\theta_2), \quad \text{(IV.12)}$$

where θ_1 is defined as above and θ_2 is analogously the angle between one of the top antiquark decay products and one of the reference directions $\hat{\mathbf{b}}$ defined in Eq. (III.7). The coefficients C_i are determined by the double spin asymmetries (III.5) and the spin analysing powers of the two decay products a_1 and

8

a_2. Finally, a non-zero expectation value of the observable defined in Eq. (III.8) leads to a distribution of the form

$$\frac{1}{\sigma}\frac{d\sigma(\gamma\gamma \to a_1 a_2 + X)}{d\cos\varphi} = \frac{1}{2}(1 - D\cos\varphi), \quad \text{(IV.13)}$$

where φ is the angle between the direction of flight of the top decay product a_1 and the antitop decay product a_2 defined in the t and $\bar{t}$ rest frames, respectively. We recall that these rest frames have to be obtained by a rotation-free boost from the $t\bar{t}$-ZMF.

The spin analysing power of the t and $\bar{t}$ decay products is encoded in the one-particle inclusive angular distributions $d\Gamma/d\cos\theta$ for the decays

$$t(s_t) \to a_1(q_1) + X_1,$$
$$\bar{t}(s_{\bar{t}}) \to a_2(q_2) + X_2. \quad \text{(IV.14)}$$

Here q_1 and q_2 are the momenta of a_1 and a_2, respectively, defined in the rest frame of the (anti)top quark. and θ is the angle between the polarization vector of the (anti)top quark and the direction of flight of $a_1(a_2)$. For a fully polarized ensemble of top quarks (antiquarks) these distributions are of the form

$$\frac{d\Gamma^{(1,2)}}{d\cos\theta} = \frac{\Gamma^{(1,2)}}{2}(1 \pm \kappa^{(1,2)}\cos\theta), \quad \text{(IV.15)}$$

where $\Gamma^{(1,2)}$ is the partial width of the respective decay channel. The quantity $\kappa^{(1,2)}$ is the (anti)top-spin analysing power of $a_{1,2}$. For the case of the standard $(V-A)$ charged current interactions these distributions were computed to order α_s for the semileptonic and non-leptonic channels in Refs. [16] and [17], respectively.

As we work to lowest order in the electroweak couplings, $\Gamma^{(2)} = \Gamma^{(1)}$ and $\kappa_2 = \kappa_1$ to all orders in α_s, if the channel $a_2 + X_2$ is the charge-conjugate of $a_1 + X_1$.

For semileptonic top decays $t \to b\ell^+\nu_\ell(g)$, the charged lepton is the most efficient analyser of the spin of the top quark. In the case of non-leptonic decays $t \to b q\bar{q}'(g)$ a good top spin analyser that can be identified easily is the least-energetic light quark jet.

In Ref. [17] the coefficients $\kappa^{(f)}$ were given to NLO accuracy for different choices of the spin analyser. To compute the coefficients B_i, C_i and D we need the partial widths

$$\Gamma^{(\text{sl,h})} = a_0^{(\text{sl,h})} + 4\pi\alpha_s a_1^{(\text{sl,h})}, \quad \text{(IV.16)}$$

where the indices sl and h stand for semileptonic and hadronic decay modes. Further, we need the dimensionful coefficients

$$\Gamma^{(\text{sl,h})}\kappa^{(\ell,j)} = b_0^{(\ell,j)} + 4\pi\alpha_s b_1^{(\ell,j)}, \quad \text{(IV.17)}$$

where ℓ (j) refers to using the charged lepton (least-energetic light quark jet) as spin analyser. For the determination of these coefficients we use the Fermi constant $G_F = 1.16639 \times 10^{-5}$ GeV^{-2}, $m = 178$ GeV, $m_W = 80.42$ GeV, $\Gamma_W = 2.12$ GeV, $m_b = 4.75$ GeV, and all other quark and lepton masses are put to zero. (We do not use the narrow width approximation for the intermediate W boson.) We obtain, putting the CKM matrix elements $|V_{tb}| = |V_{qq'}| = 1$:

$$a_0^{\text{h}} = 0.52221 \text{ GeV},$$

$$
\begin{aligned}
a_0^{\mathrm{sl}} &= \frac{a_0^{\mathrm{h}}}{N}, \\
a_1^{\mathrm{h}} &= -0.01968(15)\,\mathrm{GeV}, \\
a_1^{\mathrm{sl}} &= -0.01097(5)\,\mathrm{GeV}.
\end{aligned}
\tag{IV.18}
$$

For the relevant coefficients $b_{0,1}$ we obtain:

$$
\begin{aligned}
b_0^{\ell} &= a_0^{\mathrm{sl}}, \\
b_0^{j} &= 0.26950\,\mathrm{GeV}, \\
b_1^{\ell} &= -0.01118(8)\,\mathrm{GeV}, \\
b_1^{j} &= -0.02375(26)\,\mathrm{GeV}.
\end{aligned}
\tag{IV.19}
$$

The Durham algorithm was used as jet clustering scheme to obtain the four parton contribution to b_1^{j}. Within the leading pole approximation for the intermediate top quarks and antiquarks, the coefficients of the single and double differential distributions (IV.11)–(IV.13) are obtained in terms of the following quantities:

$$
\begin{aligned}
\sigma_s &= \frac{\alpha^2 Q_t^4}{m^2}\frac{1}{\Gamma_t}\int_0^{y_{\max}}dy_1\int_0^{y_{\max}}dy_2 f_\gamma^e(y_1,P_e,P_L)f_\gamma^e(y_2,P_e,P_L) \\
&\quad \times \left\{ c^{(0)}a_0^{(1)} + 4\pi\alpha_s\left[c^{(1)}a_0^{(1)} + c^{(0)}a_1^{(1)}\right]\right\},
\end{aligned}
\tag{IV.20}
$$

$$
\begin{aligned}
\sigma_d &= \frac{\alpha^2 Q_t^4}{m^2}\frac{1}{\Gamma_t^2}\int_0^{y_{\max}}dy_1\int_0^{y_{\max}}dy_2 f_\gamma^e(y_1,P_e,P_L)f_\gamma^e(y_2,P_e,P_L) \\
&\quad \times \left\{ c^{(0)}a_0^{(1)}a_0^{(2)} + 4\pi\alpha_s\left[c^{(1)}a_0^{(1)}a_0^{(2)} + c^{(0)}a_1^{(1)}a_0^{(2)} + c^{(0)}a_0^{(1)}a_1^{(2)}\right]\right\},
\end{aligned}
\tag{IV.21}
$$

$$
\begin{aligned}
N_r^s &= \frac{\alpha^2 Q_t^4}{m^2}\frac{1}{\Gamma_t}\int_0^{y_{\max}}dy_1\int_0^{y_{\max}}dy_2 f_\gamma^e(y_1,P_e,P_L)f_\gamma^e(y_2,P_e,P_L) \\
&\quad \times \left\{ d_r^{(0)}b_0^{(1)} + 4\pi\alpha_s\left[d_r^{(1)}b_0^{(1)} + d_r^{(0)}b_1^{(1)}\right]\right\},
\end{aligned}
\tag{IV.22}
$$

$$
\begin{aligned}
N_r^d &= \frac{\alpha^2 Q_t^4}{m^2}\frac{1}{\Gamma_t^2}\int_0^{y_{\max}}dy_1\int_0^{y_{\max}}dy_2 f_\gamma^e(y_1,P_e,P_L)f_\gamma^e(y_2,P_e,P_L) \\
&\quad \times \left\{ d_r^{(0)}b_0^{(1)}b_0^{(2)} + 4\pi\alpha_s\left[d_r^{(1)}b_0^{(1)}b_0^{(2)} + d_r^{(0)}b_1^{(1)}b_0^{(2)} + d_r^{(0)}b_0^{(1)}b_1^{(2)}\right]\right\}.
\end{aligned}
\tag{IV.23}
$$

We then get to NLO in α_s:

$$
\mathrm{D} = \frac{N_1^d}{\sigma_d}, \qquad \mathrm{C_{heli}} = \frac{N_2^d}{\sigma_d}, \qquad \mathrm{C_{beam}} = \frac{N_3^d}{\sigma_d}, \qquad \mathrm{B_{heli}} = \frac{N_4^s}{\sigma_s}, \qquad \mathrm{B_{beam}} = \frac{N_5^s}{\sigma_s}.
\tag{IV.24}
$$

The LO and NLO results for these quantities are shown in Table 2 for favorable and realistic choices of electron and laser polarizations, using the same parameters as in Table 1. In most cases the QCD corrections are of the order of a few percent and thus much smaller than the corrections to the total $t\bar{t}$ cross section. This was to be expected, since the bulk of the corrections is due to soft gluons which do

not affect the $t\bar{t}$ spin state. The biggest correction ($\sim 11\%$) occurs for the coefficient B_{beam} if the least energetic light jet is used as spin analyser.

Photon polarization is an important asset: It is necessary to obtain polarized top quarks and thus non-zero coefficients B_{heli} and B_{beam}. Further, the choice $(P_{e1}, P_{e2}; P_{L1}, P_{L2}) = (0.85, 0.85; -1, -1)$, which increases the total yield of $t\bar{t}$ pairs by more than a factor of 3 (see Table 1), in addition leads to larger $t\bar{t}$ spin correlations. In particular, in the helicity basis the correlation is then almost 100% in the dilepton channel.

Table 2: *Results for double and single spin asymmetries at $\sqrt{s_{ee}} = 500$ GeV.*

		dilepton		lepton-jet		jet-jet	
	$(P_{e1}, P_{e2}; P_{L1}, P_{L2})$	LO	NLO	LO	NLO	LO	NLO
D	$(0, 0; 0, 0)$	-0.670	-0.686	-0.346	-0.338	-0.178	-0.167
	$(0.85, 0.85; -1, -1)$	-0.806	-0.801	-0.416	-0.394	-0.215	-0.194
C_{heli}	$(0, 0; 0, 0)$	0.811	0.826	0.418	0.408	0.216	0.201
	$(0.85, 0.85; -1, -1)$	0.985	0.981	0.508	0.483	0.262	0.238
C_{beam}	$(0, 0; 0, 0)$	-0.580	-0.606	-0.299	-0.299	-0.154	-0.148
	$(0.85, 0.85; -1, -1)$	-0.808	-0.804	-0.417	-0.396	-0.215	-0.195
		lepton+X		jet+X			
	$(P_{e1}, P_{e2}; P_{L1}, P_{L2})$	LO	NLO	LO	NLO		
B_{heli}	$(0.85, 0.85; -1, -1)$	0.658	0.655	0.340	0.323		
B_{beam}	$(0.85, -0.85; -1, 1)$	-0.684	-0.637	-0.353	-0.314		

So-called non-factorizable corrections do neither contribute at NLO QCD to $\sigma_{t\bar{t}}$ nor to the angular correlations considered above. A proof of this statement is given in [15].

V. Conclusions

We have computed a variety of spin observables for the process $\gamma\gamma \to t\bar{t}X$ up to order $\alpha^2 \alpha_s$. Together with the differential rates of polarized top and antitop quark decays at order α_s, we have obtained the NLO QCD contributions to the fully differential cross section with intermediate top quark pair production at a photon collider.

We have applied the above results to $t\bar{t}$ production and decay at a future linear collider operating at $\sqrt{s} = 500$ GeV. We have shown that for an appropriate choice of the polarizations of the laser and electron beam, the cross section and the double/single spin asymmetries can be quite large. While the QCD corrections to the cross section can be very large, most of the double/single spin asymmetries are affected at the level of only a few percent. The observables considered here will provide useful

tools to analyse in detail the top quark pair production and decay dynamics. In particular, their precise measurement will test whether the top quark truly behaves as a quasi-free fermion as predicted in the Standard Model.

Acknowledgments

References

[1] I. F. Ginzburg, G. L. Kotkin, S. L. Panfil, V. G. Serbo and V. I. Telnov, Nucl. Instrum. Meth. A **219** (1984) 5.

[2] S. J. Brodsky, P. M. Zerwas, Nucl. Instrum. Meth. A **355** (1995) 19.

[3] B. Badelek *et al.* [ECFA/DESY Photon Collider Working Group], Int. J. Mod. Phys. A **19** (2004) 5097 [arXiv:hep-ex/0108012].

[4] M. Drees, M. Kramer, J. Zunft and P. M. Zerwas, Phys. Lett. B **306** (1993) 371.

[5] J. H. Kuhn, E. Mirkes and J. Steegborn, Z. Phys. C **57** (1993) 615.

[6] G. Jikia and A. Tkabladze, Phys. Rev. D **54** (1996) 2030 [arXiv:hep-ph/9601384].

[7] G. Jikia and A. Tkabladze, Phys. Rev. D **63**, 074502 (2001) [arXiv:hep-ph/0004068].

[8] A. Denner, S. Dittmaier and M. Strobel, Phys. Rev. D **53** (1996) 44 [arXiv:hep-ph/9507372].

[9] S. Y. Choi and K. Hagiwara, Phys. Lett. B **359**, 369 (1995) [arXiv:hep-ph/9506430].

[10] B. Grzadkowski, Z. Hioki, K. Ohkuma and J. Wudka, Nucl. Phys. B **689** (2004) 108 [arXiv:hep-ph/0310159]; Phys. Lett. B **593**, 189 (2004) [arXiv:hep-ph/0403174].

[11] H. Anlauf, W. Bernreuther and A. Brandenburg, Phys. Rev. D **52** (1995) 3803 [Erratum-ibid. D **53** (1996) 1725] [arXiv:hep-ph/9504424].

[12] W. Bernreuther, A. Brandenburg and M. Flesch, Phys. Rev. D **56** (1997) 90 [arXiv:hep-ph/9701347].

[13] V. S. Fadin, V. A. Khoze and M. I. Kotsky, Z. Phys. C **64** (1994) 45 [arXiv:hep-ph/9403246].

[14] W. Bernreuther, J. P. Ma and B. H. J. McKellar, Phys. Rev. D **51** (1995) 2475 [arXiv:hep-ph/9404235].

[15] W. Bernreuther, A. Brandenburg, Z. G. Si and P. Uwer, Nucl. Phys. B **690** (2004) 81 [arXiv:hep-ph/0403035].

[16] A. Czarnecki, M. Jezabek and J. H. Kühn, Nucl. Phys. B **351** (1991) 70.

[17] A. Brandenburg, Z. G. Si and P. Uwer, Phys. Lett. B **539** (2002) 235 [arXiv:hep-ph/0205023].